J. MACROMOL. SCI.—PHYS., B39(5&6), 775–792 (2000)

A New Technique for Using DSC Melting Endotherms to Study Isothermal Bulk Crystallization of Semicrystalline Polymers at Low Degrees of Undercooling: Syndiotactic Polypropylene*

PITT SUPAPHOL[1,†] and JOSEPH E. SPRUIELL[2]
[1]The Petroleum and Petrochemical College
Chulalongkorn University
Bangkok 10330, Thailand
[2]Materials Science and Engineering
University of Tennessee
Knoxville, TN 37996

ABSTRACT

In this manuscript, we present a new technique for using a differential scanning calorimeter (DSC) to study isothermal bulk crystallization and the kinetics of the process at "high" crystallization temperatures or "low" degrees of undercooling. It is based on measurements of the enthalpy of fusion from the subsequent melting endotherms after isothermal crystallization for various time intervals. Syndiotactic polypropylene (s-PP) was used as the model system. The benefits of the new technique, based on the results we present here, are threefold: (1) it allows an accurate determination of the induction time; (2) it offers a means to extend the use of DSC to obtain kinetics parameters for isothermal crystallization at temperatures at which the traditional technique is not applicable; and (3)

*This manuscript is dedicated to the memory of Professor Donald C. Bogue.
†To whom correspondence should be addressed. E-mail: ps@sunsv1.ppc.chula.ac.th

it gives an insight into certain mechanistic aspects of the isothermal crystallization process as it occurs at different crystallization time intervals.

Key Words. Avrami analysis, Crystallization kinetics, Crystallization and melting behavior, DSC, Syndiotactic polypropylene.

INTRODUCTION

Differential scanning calorimetry (DSC) is an excellent tool for following thermal transitions of polymers. Much of the historical significance and many of the applications of DSC, as a thermal analytical device, can be found in an excellent monograph by Wunderlich [1]. Various uses of DSC related to the studies of crystallization and subsequent melting processes of semicrystalline polymers can be summarized as follows [2–4]:

1. To determine thermodynamic properties associated with the crystallization process (e.g., crystallization temperature T_c, enthalpy of crystallization ΔH_c, etc.) and related kinetics parameters (e.g., the half-time of crystallization $t_{0.5}$, etc.) of the process under both isothermal and nonisothermal conditions.
2. To determine thermodynamic properties associated with the melting process (e.g., melting temperature T_m, enthalpy of fusion ΔH_f, etc.) and the kinetics of the melting process.
3. To determine the final apparent degree of crystallinity $\chi_{c,\infty}$ in polymer samples after crystallization at conditions of interest.

In this manuscript, we focus on using DSC to study the crystallization, including the kinetics of the process, and subsequent melting behavior of semicrystalline polymers under isothermal conditions. Traditionally, studies of isothermal crystallization kinetics of polymers by DSC have been based on the information obtained from the crystallization exotherms [2–4]. Though proven to be a very quick and efficient technique, utilization of crystallization exotherms in studying crystallization kinetics can only be applied under certain conditions for which the signal can be detected reliably by the instrument. In other conditions, Hay and colleagues [2,4] suggested an alternative technique in which subsequent melting endotherms were used to study crystallization kinetics.

Surprisingly, despite being suggested by Hay and colleagues [2,4] over 20 years ago, the technique for using subsequent melting endotherms in studying crystallization of semicrystalline polymers, to the best of our knowledge, has never been used directly to obtain kinetics parameters in a real polymer system. Therefore, in the present manuscript, we critically analyze the use of subsequent melting endotherms in studying isothermal crystallization, including the kinetics of the process, and subsequent melting behavior of semicrystalline polymers using syndiotactic polypropylene (s-PP) as our model material. We demonstrate that the new technique may be suitable for studying crystallization kinetics of certain semicrystalline polymers at "high" crystallization temperatures (or "low" degrees of undercooling) for which the traditional technique is not applicable. Reliability and applicability of the new technique will be tested by comparing, based on measurements carried out at some temperatures at which both techniques can be applied, the experimental results with those obtained from the standard technique.

MARCEL DEKKER, INC.
270 Madison Avenue, New York, New York 10016

USE OF DIFFERENTIAL SCANNING CALORIMETRY IN STUDYING CRYSTALLIZATION OF POLYMERS

General Technique

Figure 1 shows a typical crystallization exotherm after complete crystallization at $T_c = 77.5°C$ (note that the sample was completely melted at 190°C for 5 min to ensure complete melting [5] before being quenched to the crystallization temperature). Crystallization is assumed to begin at point A, which is preceded by a short period in which the temperature of the sample is equilibrated to T_c. Increasing heat flow as a result of exothermic energy during evolution of the crystallinity (i.e., enthalpy of crystallization) is evident until a maximum is observed at point B. The rate of evolution of the crystallinity depends strongly on the kinetics of the crystallization process, which is very sensitive to changes in crystallization temperature T_c. After point B, crystallization slows significantly, and the measurement is terminated (i.e., at point C) when no noticeable change in the heat flow is detected.

Intuitively, during crystallization of semicrystalline polymers under isothermal conditions, it is assumed that the observed heat flow is directly proportional to the weight of the sample w, the enthalpy of crystallization ΔH_c, and the instantaneous crystallization rate $\dot{\theta}(t)$. The enthalpy of crystallization is a multiplication product of the final degree of crystallinity $\chi_{c,\infty}$ and the enthalpy of crystallization of an infinitely thick crystal ΔH_c^0 (i.e., 100% crystalline sample). Consequently, we may write an equation for the heat flow as

$$\dot{Q} = c_1 \cdot w \cdot \chi_{c,\infty} \cdot \Delta H_c^0 \cdot \dot{\theta}(t) \tag{1}$$

where c_1 is a combined physical constant specific for each DSC used.

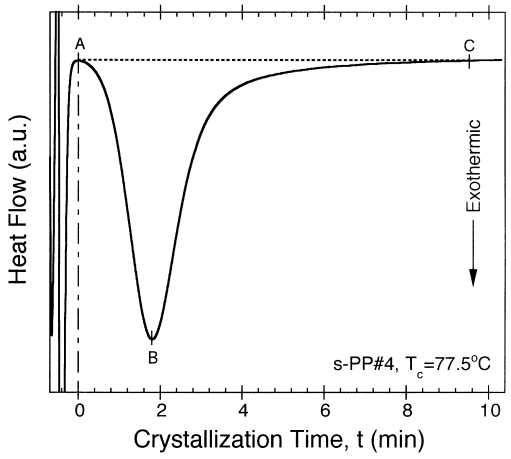

FIG. 1. Typical crystallization exotherm data of s-PP sample isothermally crystallized at $T_c = 77.5°C$.

By setting $\dot{q} = \dot{Q}/(c_1 \cdot w \cdot \chi_{c,\infty} \cdot \Delta H_c^0)$, the relative crystallinity $\theta(t)$ can be obtained by integration of the transient normalized heat flow $\dot{q}(t)$ over the course of the crystallization. One finally obtains

$$\theta(t) = \int_0^t \dot{\theta}(t')dt' = \int_0^t \dot{q}(t')dt' \tag{2}$$

Figure 2 shows a plot of relative crystallinity $\theta(t)$ as a function of crystallization time t calculated from the heat flow data shown in Fig. 1 according to Eq. 2. An important parameter, which can be obtained very easily from the relative crystallinity plot similar to Fig. 2, is the half-time of crystallization $t_{0.5}$; it is defined as the time spent from the onset of the crystallization to the point at which the crystallization is 50% complete. It should be noted that the reciprocal of the crystallization half-time (i.e., $t_{0.5}^{-1}$) is often used to characterize the overall rate of the crystallization process.

Even though DSC has been used successfully to follow crystallization of semicrystalline polymers through crystallization exotherms, a number of limitations associated with the instrument itself need to be discussed. Since what DSC really measures during the course of crystallization is the rate of evolution of exothermic energy, as mentioned previously, the technique is limited intuitively by the sensitivity of the detectors, which somewhat varies from one instrument to another. One of the most important limitations occurs in the use of DSC to study isothermal crystallization of polymers at high crystallization temperatures T_c (or at low degrees of undercooling ΔT, defined as $T_m^0 - T_c$). Under such conditions, the signal-to-noise ratio becomes too small, causing a problem for the determination of the baseline in the signal obtained. Without a proper baseline, the following problems may arise: (1) inaccuracy in the determination of the onset of crystallization and hence inaccuracy in the determination of the induction period t_0; and (2) incorrect conversion of the experimental data to the relative crystallinity $\theta(t)$, hence causing dubious crystallization kinetics parameters to be obtained.

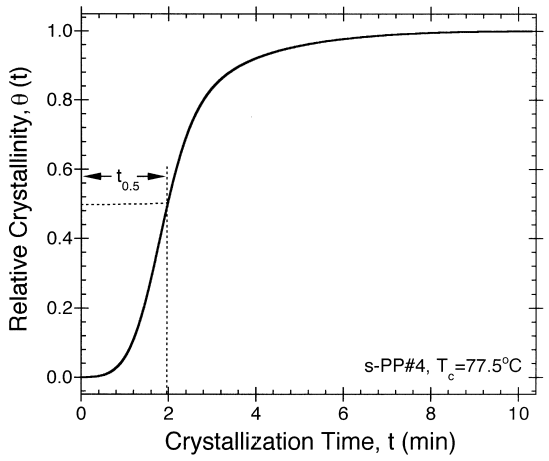

FIG. 2. Typical relative crystallinity $\theta(t)$ as a function of crystallization time t calculated from the raw data shown in Fig. 1 according to Eq. 2.

MARCEL DEKKER, INC.
270 Madison Avenue, New York, New York 10016

Due to the aforementioned limitations, the traditional technique for using DSC to follow crystallization of semicrystalline polymers can only be applied within a limited range of crystallization temperatures for which the total time for the completion of crystallization does not take too long (this is limited greatly by the sensitivity of the DSC being used). To overcome this particular problem, it will be demonstrated here that it is possible to extend the use of DSC to follow crystallization of polymers at high crystallization temperatures T_c (or low degrees of undercooling ΔT) by measuring the enthalpy of fusion $\Delta H_{f,t}$ of crystallites developed at T_c after isothermal crystallization for various time intervals.

As a first approximation, it is assumed that the crystallization at T_c ends when there is no significant change being observed in the $\Delta H_{f,t}$ value after a sample is crystallized completely. This can be presented mathematically by thinking that the time of crystallization at T_c approaches infinity; that is,

$$\lim_{t\to\infty}\Delta H_{f,t} = \Delta H_{f,\infty} \tag{3}$$

where $\Delta H_{f,\infty}$ denotes the final value of enthalpy of fusion of the crystallites formed at T_c. As a result of this assumption (i.e., Equation 3), it is possible to calculate the relative crystallinity $\theta(t)$ according to the following equation:

$$\theta(t) = \Delta H_{f,t}/\Delta H_{f,\infty} \tag{4}$$

which will be used for further analysis using an appropriate macrokinetic model.

Determination of Crystallization Kinetics Parameters

In addition to the half-time of crystallization $t_{0.5}$ and its reciprocal value $t_{0.5}^{-1}$, which can be determined directly from the experimental plot of relative crystallinity $\theta(t)$ as a function of crystallization time t, other kinetics parameters can also be determined using an appropriate macrokinetic model. For the purpose of describing the macroscopic evolution of primary crystallinity under quiescent isothermal conditions, three major macrokinetic models have been proposed thus far. They are (1) the "Avrami" model [6–12], (2) the Tobin model [13–15], and (3) the Malkin model [16]. Since critical comparison among the three models in describing the primary crystallization of polymers (in the case of s-PP, see Ref. 17) is not our prime concern in this manuscript, only the well-known Avrami model is used to analyze the experimental data.

Based primarily on the notion of microscopic mechanisms of primary nucleation and subsequent crystal growth, the Avrami equation describing steady-state isothermal phase transformation is given by [6–12]

$$\theta(t) = \frac{\chi_{c,t}}{\chi_{c,\infty}} = 1 - \exp(-k_a t^{n_a}) \tag{5}$$

where $\theta(t)$ denotes the relative crystallinity as a function of time (see Eq. 2), $\chi_{c,t}$ is the apparent degree of crystallinity at an arbitrary time t during the course of the crystallization process, $\chi_{c,\infty}$ is the final apparent degree of crystallinity, k_a is the Avrami crystallization rate constant, and n_a is the Avrami exponent of time. Both n_a and k_a are constants typical of a given crystalline morphology and type of nucleation for a particular crystallization condition [18].

MARCEL DEKKER, INC.
270 Madison Avenue, New York, New York 10016

According to the original assumptions of the theory, the value of n_a should be integral, ranging from 1 to 4 [8–10]. Analysis of the experimental data based on the Avrami equation, in most cases, however, leads to fractional values of the Avrami exponent n_a. Possible explanations for this discrepancy were given elsewhere [17]; the nonintegral observations of the Avrami exponent n_a may be explained based on the simultaneous Avrami model [17,19], which was postulated based on observations of dual transient nucleation mechanisms (i.e., instantaneous and sporadic nucleation) and the Ding-Spruiell version of the Avrami equation [12]. The latter accounts for the fractional values of n_a through the introduction of the nucleation index [12], which may quantify the nucleation mechanisms much better than the use of the simultaneous Avrami model.

Analysis of the experimental data based on the Avrami equation is straightforward. The Avrami kinetics parameters k_a and n_a can be extracted graphically from a least-square line fitted to the double logarithmic plot of $\ln\{-\ln[1-\theta(t)]\}$ versus $\ln(t)$, where k_a is taken as the antilogarithmic value of the y intercept, and n_a is the slope of the least-square line. Normally, the kinetics parameters are calculated from the least-square line drawn through the bulk of the data in the range of $\theta(t) \in [0.10, 0.80]$ (where a straight-line portion is observed). An alternative method for extracting the kinetics parameters is to fit the experimental data directly to the appropriate macrokinetic model using a nonlinear multivariable regression program (i.e., the data-fitting method); this has proven to be a fast, effective, and reliable method for determining the kinetics data [17].

EXPERIMENTAL

Materials

The metallocene s-PP sample (in this work, s-PP#4) used in this study was supplied in pellet form by Fina Oil and Chemical Company of La Porte, Texas. Molecular characterization data, which were kindly performed by Dr. Roger A. Phillips and his group at Montell USA, Incorporated, in Elkton, Maryland, shows the following molecular weight information: $M_n = 81{,}300$ daltons, $M_w = 171{,}000$ daltons, $M_z = 294{,}000$ daltons, and $M_w/M_n = 2.1$. In addition, the syndiotacticity measured by ^{13}C nuclear magnetic resonance (NMR) shows the racemic dyad content [*%r*] to be 89.2%, the racemic triad content [*%rr*] to be 84.4%, and the racemic pentad content [*%rrrr*] to be 74.6%.

Sample Preparation

Sliced pellets were melt pressed at about 4.6×10^2 MN·m^{-2} between a pair of polyimide films, which in turn were sandwiched between a pair of thick metal plates in a Wabash compression-molding machine preset at a temperature of 190°C. After a 10-min holding time at the preset condition, a film about 290 μm thick was taken out and allowed to cool at ambient condition to room temperature between the two metal plates. This treatment assumes that previous thermomechanical history was essentially erased and provides a standard crystalline memory condition for our experiments.

Technique and Experimental Methods

A DSC-7 (Perkin-Elmer) was used to follow the isothermal crystallization and subsequent melting behavior of s-PP. The DSC, equipped with an internal liquid nitrogen cooling unit, reliably provided a cooling rate up to 200°C·min^{-1}. Temperature calibration

was performed using a pure indium standard ($T_m^0 = 156.6°C$ and $\Delta H_f^0 = 28.5\ J \cdot g^{-1}$). Calibration of the temperature scale was performed every other run to ensure the accuracy and reliability of the data obtained. To make certain that thermal lag between the polymer sample and the DSC sensors was kept to a minimum, each sample holder was loaded with a single disk weighing 7.1 ± 0.3 mg, which was cut from the standard as-prepared film. Each sample was used only once, and all the runs were carried out under nitrogen purge.

To use DSC to follow the crystallization behavior of polymers at high crystallization temperatures T_c, the new technique for measuring the enthalpy of fusion $\Delta H_{f,t}$ in subsequent melting endotherms after isothermal crystallization for various time intervals at T_c were used in this study. Even though the purpose of the technique is to use DSC to study crystallization behavior of s-PP at high T_c values, it was also applied to observe crystallization behavior and the kinetics of the process at moderate T_c values of 75°C, 90°C, and 95°C to compare with the results obtained previously [20] based on the traditional technique. The new technique was finally applied to study crystallization behavior and its kinetics for $T_c = 100°C$ and 105°C, which cannot be studied in the DSC when the traditional technique is used primarily due to the low signal-to-noise ratio observed in the heat flow data. Experimental data were analyzed based on the Avrami equation (see Eq. 5) using the data-fitting method [17].

For a given crystallization temperature T_c, samples were heated from room temperature at $80°C \cdot min^{-1}$ to 190°C, at which they were kept for 5 min to ensure complete melting [5]. The samples were then quenched to T_c, at which they were left for crystallization. After a certain crystallization time interval at T_c, the samples were immediately heated at $20°C \cdot min^{-1}$ to 190°C, while the subsequent melting endotherm was recorded for further analysis.

RESULTS AND DISCUSSION

Origin of the New Technique

Figure 3 illustrates some representative DSC melting thermograms of s-PP#4 after isothermal crystallization at $T_c = 75°C$ for 1.0, 1.5, 1.7, 2.0, 2.5, and 8.0 min. Figure 4 shows DSC melting thermograms after isothermal crystallization at $T_c = 95°C$ for 15, 20, 25, 30, 40, and 50 min. The heating rate used in all of the scans was $20°C \cdot min^{-1}$. At $T_c = 75°C$, a time interval of at least 0.5 min was required for a melting peak just to be observed in the subsequent melting endotherm (not shown). Similarly, a time period of at least 5 min was needed for a melting peak to be observed in the subsequent melting endotherm after isothermal crystallization at $T_c = 95°C$. To a first approximation, the time intervals of about 0.5 and 5 min correspond to the induction time t_0 needed for stable crystallites to be formed at $T_c = 75°C$ and 95°C, respectively. It should be kept in mind that accuracy of the observed induction time is likely to vary from one technique (and its sensitivity) to another. In principle, it may be possible to determine the induction time t_0 more accurately by varying the crystallization time interval in a small step increment, but it is a rather tedious task and may not be necessary if the accurate t_0 value is not of prime concern.

Another interesting phenomenon that can be observed directly from plots of melting thermograms after isothermal crystallization at various time intervals is the occurrence of secondary crystallization. At $T_c = 75°C$, a small endotherm (denoted as the minor

MARCEL DEKKER, INC.
270 Madison Avenue, New York, New York 10016

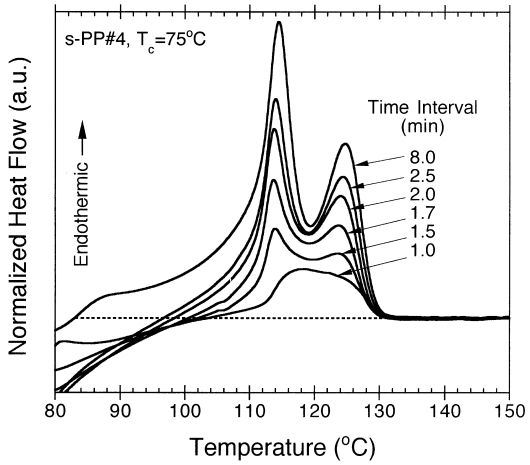

FIG. 3. DSC subsequent melting endotherms (20°C·min^{-1}) of s-PP sample isothermally crystallized at $T_c = 75$°C for different time intervals as indicated.

endotherm) located at about 87°C is clearly discernible in the DSC thermogram after isothermal crystallization for 8 min, while at $T_c = 95$°C, small endotherms are apparent at about 107°C after isothermal crystallization for 40 and 50 min. Careful examination of all of the recorded DSC thermograms, however, shows that the appearance of the minor endotherms in the DSC thermograms was not clearly observed until an approximate crystallization time interval of 4 min at $T_c = 75$°C was reached, whereas it was about 25 min at $T_c = 95$°C. The position at which the minor endotherm is observed in a

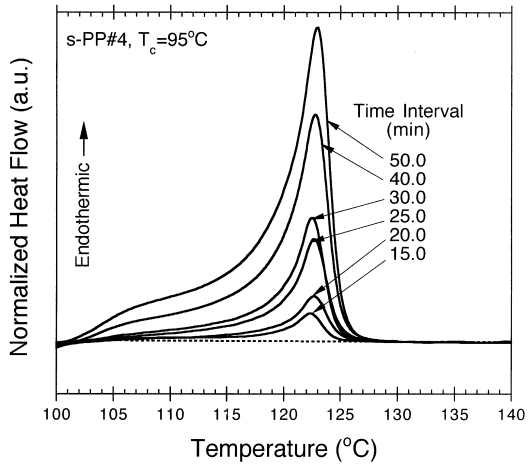

FIG. 4. DSC subsequent melting endotherms (20°C·min^{-1}) of s-PP sample isothermally crystallized at $T_c = 95$°C for different time intervals as indicated.

subsequent melting scan is also interesting as it always appears close to the temperature at which the sample was crystallized (ca. $T_c + 10°C$).

The facts that the small endotherm (1) is usually observed at a temperature close to the crystallization temperature, (2) is observed at a later stage of crystallization, and (3) increases in its magnitude and possibly shifts to higher temperature with increasing crystallization time suggest that the small endotherm is a result of the contributions from a rather slow crystallization mechanism occurring at T_c, which is likely to be a result of the secondary crystallization. Observation of the small endothermic shoulder is not limited to the case of s-PP. A number of investigators have reported similar observations in various polymer systems, such as poly(ethylene terephthalate) (PET) [21] and poly(butylene naphthalate terephthalate) (PBNT) copolyesters [22].

Additional important information that can be observed directly from plots of melting thermograms after isothermal crystallization at various time intervals is whether a lamellar thickening process occurs during crystallization in the polymer system studied. In principle, this information can be deduced readily from the position(s) of the primary melting peak(s), which correspond(s) to the primary crystalline aggregates formed during primary crystallization at T_c based on the Gibbs-Thomson equation [23], which correlates the observed melting temperature T_m to the lamellar thickness of the crystallites. The equation is given by

$$T_m = T_m^0 \left(1 - \frac{2\sigma_e}{\Delta H_f^0} \cdot \frac{1}{l_c} \right) \tag{6}$$

where T_m^0 is the equilibrium melting temperature (i.e., the melting point of an infinitely thick crystal) of the polymer studied, σ_e is the fold surface free energy, l_c is the lamellar thickness, and ΔH_f^0 is the equilibrium enthalpy of fusion.

It is clearly seen from Figs. 3 and 4 that the positions of the primary melting peak in the subsequent melting endotherms recorded at various time intervals were essentially unchanged, exhibiting average values of $114.1°C \pm 0.2°C$ for $T_c = 75°C$ and of $123.2°C \pm 0.1°C$ for $T_c = 95°C$. According to Eq. 6, this can only be construed by assuming that the thickness of the primary s-PP crystallites formed at T_c is essentially constant throughout the crystallization process. This finding agrees extremely well with the observations reported on crystallization behavior of s-PP using real-time small-angle X-ray scattering (SAXS) and DSC techniques [24–26] in which the original lamellar thickness of s-PP was proved to be constant during both isothermal crystallization and subsequent heating to the melting point.

One also needs to consider the high T_m peak in Fig. 3. We have shown, in a recent report [27] on the same resin, that for samples isothermally crystallized at $T_c \leq 90°C$, three melting endotherms are observed, while only two melting endotherms are present in samples isothermally crystallized at $T_c \geq 95°C$. Based mainly on DSC and X-ray diffraction techniques, the results suggested that the minor endotherm represents the melting of the secondary crystallites formed at T_c. The low-temperature melting endotherm (viz. the main melting endotherm) corresponds to the melting of the primary crystallites formed at T_c, while the high-temperature melting endotherm was attributed to the melting of the crystallites recrystallized during a heating scan (i.e., remelting phenomenon). Thus, the presence of the melting endotherm at about 125°C of s-PP samples isothermally crystallized at $T_c = 75°C$ (see Fig. 3) is clearly a result of the remelting phenomenon.

The subsequent melting endotherms recorded after isothermal crystallization at various time intervals in studying the crystallization behavior of s-PP were shown above. We now show that the new technique can also be used to obtain related crystallization kinetics information. Figure 5 shows the relative crystallinity data $\theta(t)$, based on the enthalpy of fusion $\Delta H_{f,t}$ as in Figs. 3 and 4, plotted as a function of time (in logarithmic scale for $T_c = 75°C$, 90°C, 95°C, 100°C, and 105°C, respectively.

Closer examination of the $\Delta H_{f,t}$ data measured from the endotherms such as those shown in Figs. 3 and 4 indicates several possible limitations of the technique. Choice of the final value of enthalpy of fusion of the crystalline aggregates formed at T_c (i.e., $\Delta H_{f,\infty}$) can greatly affect the accuracy of the conversion of the $\Delta H_{f,t}$ data to the relative crystallinity $\theta(t)$. The fact that certain types of secondary crystallization (e.g., crystal perfection and/or lamellar thickening) are slow processes (the mechanisms and the kinetics of these processes are strongly dependent on the type of polymers) that cause a gradual increase in the observed enthalpy of fusion with time makes decisive determination of the final enthalpy of fusion $\Delta H_{f,\infty}$ difficult. The problem is even worse in the cases for which crystallization occurs at a very high temperature (or low degree of undercooling) since the majority of the crystallinity within a growing crystalline aggregate is due to the secondary crystallization process.

In addition, the procedure used to measure the enthalpy of fusion $\Delta H_{f,t}$ from a melting endotherm poses another possible problem to the accuracy and reliability of the relative crystallinity data $\theta(t)$ obtained. We measured the enthalpy of fusion by determining the area under the melting endotherm curve. The baseline used was taken as the line drawn parallel to the heat capacity of the polymeric melt (shown in Figs. 3 and 4 as the dotted line). For the technique to be reliable, the procedure used to measure $\Delta H_{f,t}$ data needs to be at least consistent throughout all of the measurements. Different procedures

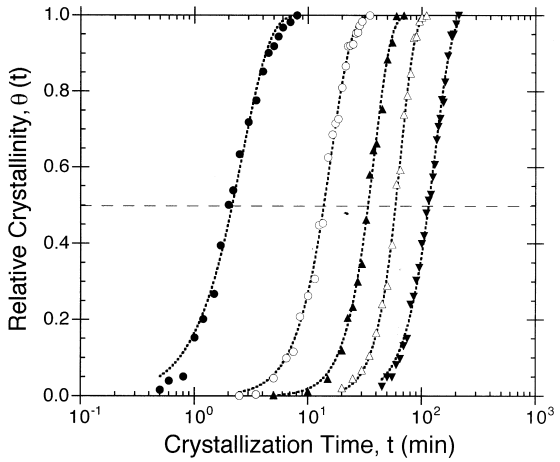

FIG. 5. Relative crystallinity $\theta(t)$ as a function of crystallization time t (in logarithmic scale) of sPP sample calculated from enthalpy of fusion $\Delta H_{f,t}$ determined from subsequent melting endotherms after isothermal crystallization for various time intervals (see Figs. 3 and 4) according to Eq. 4 for five different crystallization temperatures T_c: ●, 75°C; ○, 90°C; ▲, 95°C; △, 100°C; and ▼, 105°C.

utilized by different experimentalists to determine the $\Delta H_{f,t}$ data will make it difficult to compare data from different laboratories. For this reason, a unified procedure, such as the one used in this manuscript, should be used throughout.

Determination of Crystallization Kinetics Parameters

It is apparent in Fig. 5 that the induction time t_0, the crystallization half-time $t_{0.5}$, and the time to reach the final crystallinity increase with increasing crystallization temperature. The induction time t_0 is normally defined as the time interval the polymeric molecules in the melt state require before stable nuclei can be formed at a particular crystallization condition; for this technique, it can be determined from the time interval needed for isothermal crystallization at T_c for a melting peak just to be observable in the subsequent melting endotherm (as described in the previous section).

The crystallization half-time $t_{0.5}$ can be determined readily from a plot of $\theta(t)$ versus time t, such as those shown in Fig. 5. Due to a relatively small number of data points acquired at each T_c, it may be necessary to curve fit the raw data before an accurate estimate of the half-time $t_{0.5}$ can be obtained. In this manuscript, we directly fitted the raw data of $\theta(t)$ versus time t to the Avrami equation (i.e., Eq. 5) using a nonlinear multivariable regression program (i.e., data-fitting method [17]). After curve fitting was performed, the crystallization half-time $t_{0.5}$ was measured. Since the Avrami crystallization kinetics parameters n_a and k_a are fitting variables, they are automatically provided by the program once the best fit is determined.

Table 1 summarizes all of the crystallization kinetics parameters determined from the data shown in Fig. 5. Related crystallization kinetics parameters (denoted in Table 1 as $t^*_{0.5}$, n^*_a, and k^*_a, determined previously based on the traditional technique using crystallization exotherms (i.e., Eq. 2) from the relative crystallinity data $\theta(t)$ measured for moderate crystallization temperatures of 75°C, 90°C, and 95°C, respectively, are also listed for comparison. It should be noted that there is a slight discrepancy between the kinetics parameters reported in Table 5 of Ref. 20 and those reported in Table 1 (i.e., $t^*_{0.5}$, n^*_a, and k^*_a), even though both of the data sets were determined directly from the crystallization exotherms, is due to the fact that those reported in Ref. 20 were determined from the least-square line fitted to the double logarithmic plot of $\ln\{-\ln[1-\theta(t)]\}$ versus $\ln(t)$, whereas those reported in Table 1 were determined using the data-fitting method [17].

TABLE 1

Induction Time t_0 and Overall Avrami Crystallization Kinetics Data for Syndiotactic Polypropylene as Determined from the Present Technique (i.e., $t_{0.5}$, n_a, k_a) and the Traditional Technique (i.e., $t^*_{0.5}$, n^*_a, k^*_a)

T_c, °C	t_0, min	$t_{0.5}$, min	n_a	k_a min^{-n}	$t^*_{0.5}$, min	n^*_a	k^*_a, min^{-n}
75	0.5	1.6	1.3	3.8×10^{-1}	1.6	2.1	2.8×10^{-1}
90	2.1	11.6	2.1	4.0×10^{-3}	9.8	2.5	2.4×10^{-3}
95	4.9	28.9	2.5	1.7×10^{-4}	30.4	2.9	3.4×10^{-5}
100	7.8	51.1	2.2	2.8×10^{-5}	—	—	—
105	21.5	92.9	3.1	4.2×10^{-6}	—	—	—

MARCEL DEKKER, INC.
270 Madison Avenue, New York, New York 10016

According to Table 1, the induction time t_0 and the crystallization half-time $t_{0.5}$ increase with increasing crystallization temperature. Since the induction time t_0 could not be measured accurately from the crystallization exotherms, comparison between the data obtained from the crystallization exotherms and those obtained from the subsequent melting endotherms after isothermal crystallization cannot be made. On the other hand, the crystallization half-times $t_{0.5}$ as determined from both techniques seem to agree very well with one another, suggesting that the new technique for using subsequent melting endotherms in studying crystallization kinetics is at least reliable and applicable to describe isothermal bulk crystallization of s-PP for the conditions studied.

In the case of the Avrami kinetics analysis, the exponent n_a for primary crystallization is found to be an increasing function of crystallization temperature (within the range studied) and ranges from 1.3 to 3.1. The most likely explanation for the increase of n_a with increasing temperature is based on the fact that the average concentration of athermal nuclei decreases tremendously as the crystallization temperature increases [17,28,29], causing an increase in the number of the homogeneous nuclei at the expense of the number of the heterogeneous nuclei. The Avrami rate constant k_a appears to be very sensitive to a change in crystallization temperature, decreasing with an increase in the temperature. This confirms that the overall rate of crystallization decreases as crystallization temperature increases. It should be noted that this observation is only valid when the temperature is in the range at which the secondary nucleation rate is the rate-determining factor (i.e., $T_c \leq$ ca. 60°C for s-PP [20]).

Further Discussion of the Temperature Dependence of the Induction Time

Recently, a theory for describing temperature dependence of nucleation induction time t_0 was proposed by Lednicky and Muchova [30–35] using the classical theories of primary nucleation [36,37] as a basis. The theory offers a way to quantify the induction time in terms of the primary nucleation theories. The original purpose of the theory was to assess the nature of primary nucleation on foreign surfaces [34,35] (e.g., fibers, fillers, etc.). Since it is known that crystallization in semicrystalline polymers often starts with primary nucleation on foreign surfaces (or on predetermined nuclei of similar chemical structures), we believe that the theory of the induction time proposed by Lednicky and Muchova [30–35] should be applicable to describe the temperature dependence of the induction time data of s-PP, as we demonstrate below.

In general, crystallization of semicrystalline polymers from the melt often starts with primary nucleation due to the presence of foreign surfaces, provided that prolonged melting is carried out to ensure complete melting. In heterogeneous nucleation (i.e., crystallization on predetermined surfaces), two mechanisms are envisaged [31,33,34]: (1) formation of the first layer on the foreign surface, which is characterized by the difference in the free energies between the crystallizing species and the surface; and (2) formation of the subsequent layers until a nucleus of critical size is established, and the growth process occurs. The induction time t_0 is the sum of the time periods for the formation of the first layer (denoted t_h) and for the formation of the subsequent layers (denoted t_s).

Since the time characteristic for each mechanism is inversely proportional to the number of segments capable of nucleation [31,33,34], the equation describing the induction time is given by

$$t_0 = t_h + t_s \tag{7}$$

in which

$$t_h = E_1 \exp\left(\frac{\Delta G_\eta}{kT_c}\right)\exp\left[\frac{16(\Delta\sigma)\sigma\sigma_e T_m^0}{kT_c(\Delta H_f^0 \Delta T)^2}\right] \tag{8}$$

$$t_s = E_2\left[\frac{2(\Delta\sigma)T_m^0}{(\Delta H_f^0 \Delta T)b_0} - 1\right]\exp\left(\frac{\Delta G_\eta}{kT_c}\right)\exp\left[\frac{4b_0\sigma\sigma_e T_m^0}{kT_c(\Delta H_f^0 \Delta T)}\right] \tag{9}$$

where E_1 and E_2 are proportionality constants, ΔG_η is the free energy barrier for the molecular transport across the phase boundary, k is the Boltzman constant, $\Delta\sigma$ is the difference in the interfacial free energy of the crystallizing species and that of the heterogeneous surface, σ is the lateral surface free energy, b_0 is the layer thickness, and other quantities are the same as previously defined.

Muchova and Lednicky [33,34] showed that, in certain circumstances, one of the constituent terms dominates. Specifically, for sufficiently "high" crystallization temperatures, when the number of subsequent layers is much higher than unity (for the nucleus to be energetically stable), the time for the formation of the first layer t_h can be neglected. In such a case, the induction time t_0 is approximated by

$$t_0 = E_2\left[\frac{2(\Delta\sigma)T_m^0}{(\Delta H_f^0 \Delta T)b_0}\right]\exp\left(\frac{\Delta G_\eta}{kT_c}\right)\exp\left[\frac{4b_0\sigma\sigma_e T_m^0}{kT_c(\Delta H_f^0 \Delta T)}\right] \tag{10}$$

For some "lower" crystallization temperatures for which the number of critical layers approaches unity, the time for the formation of subsequent layers t_s can be neglected. The induction time t_0 is therefore given by

$$t_0 = E_1 \exp\left(\frac{\Delta G_\eta}{kT_c}\right)\exp\left[\frac{16(\Delta\sigma)\sigma\sigma_e T_m^0}{kT_c(\Delta H_f^0 \Delta T)^2}\right] \tag{11}$$

It should be noted that, in practice, the transport term $\exp(\Delta G_\eta/kT_c)$ is often approximated by the William-Landels-Ferry (WLF) equation for viscous flow:

$$\exp\left(\frac{\Delta G_\eta}{kT_c}\right) = \exp\left[\frac{U^*}{R(T_c - T_\infty)}\right] \tag{12}$$

where U^* is the activation energy for the diffusion of molecular segments across the melt/solid surface boundary and is commonly given by a universal value of 6276 J·mol^{-1} [23], R is the universal gas constant, and T_∞ is the temperature at which long-range molecular motion ceases and is often taken to be about 30 K or 50K below the glass transition temperature T_g (ca. –6.1°C for s-PP [20]) of the polymer of interest.

To approximate the transport term with the WLF expression (i.e., Eq. 12) and to account for a temperature dependence of the enthalpy of fusion, Eqs. 10 and 11 can be written in a more general form as

$$t_0(T_c) = \frac{\tau_1^I}{(\Delta T)f}\exp\left[\frac{U^*}{R(T_c - T_\infty)} + \frac{K_1^I}{T_c(\Delta T)f}\right] \tag{13}$$

and

$$t_0(T_c) = \tau_2^I \exp\left[\frac{U^*}{R(T_c - T_\infty)} + \frac{K_2^I}{T_c(\Delta T)^2 f^2}\right] \tag{14}$$

respectively, where τ_1^I and τ_2^I are combined preexponential terms, K_1^I and K_2^I are combined factors related to nucleation mechanism, and f is a factor used to correct for the temperature dependence of the enthalpy of fusion, that is, $f = 2T_c/(T_m^0 + T_c)$ [38].

Figure 6 illustrates the relationship of the induction time t_0 as a function of crystallization temperature. Within the temperature range studied, the induction time t_0 increases monotonically with increasing crystallization temperature. This can be explained based on the fact that, as the crystallization temperature increases, the energy barrier for molecular segments in the melt state to form stable clusters of nuclei increases significantly, thus requiring longer induction periods. To describe the temperature dependence of the observed induction time t_0, the experimental data were fitted to the approximate equations for both high and low temperature regimes (i.e., Eqs. 13 and 14, respectively) using the nonlinear multivariable regression program (shown in Fig. 6 as lines 1 and 2, respectively). Even though Eq. 13 seems to give a better fit at the lower end of the data range (i.e., $75°C \le T_c \le 90°C$), both equations can be used to describe the temperature dependence of the incubation time data in the higher temperature range (i.e., $90°C \le T_c \le 105°C$) very well.

Interestingly, both equations predict the temperature dependence of the induction time t_0 as having a U-shaped curve. This characteristic is mainly mandated by the two exponential terms. The first exponential term, $\exp[U^*/R(T_c - T_\infty)]$, corresponds to the diffusion of polymer molecules or segments from the equilibrium melt across the interfacial boundary onto a growth face. The second term, $\exp[K_i^I/T_c(\Delta T)^i f^i]$ (where i equals 1 for Eq. 13 or 2 for Eq. 14), relates to the formation of the critical nuclei on the growth face. Intuitively, due to the competing nature of the two exponential terms, a minimum in the composite curve is expected to be observed somewhere between T_∞ and T_m^0 (ca. 168.7°C for s-PP [20]). Indeed, a minimum in the fitted curves is evident in Fig. 6 at

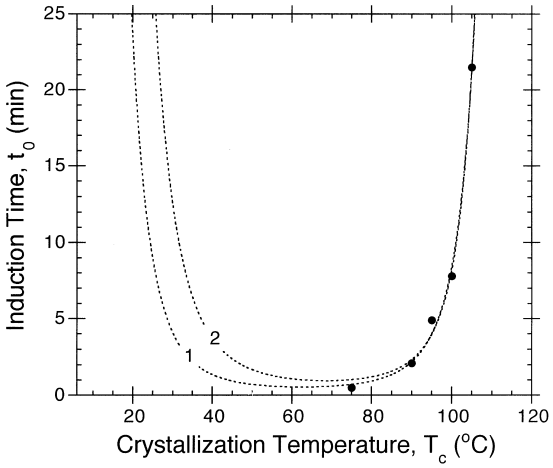

FIG. 6. Induction time t_0 (see Table 1) as a function of crystallization temperature T_c of s-PP. Dotted line 1 is the best-fitted curve drawn through the bulk of the data after Eq. 13, while dotted line 2 is drawn after Eq. 14. Parameters of the fitted curves: $\tau_1^I = 2.64 \times 10^{-8}$ min·K, $K_1^I = 4.31 \times 10^5$ K^2, $\tau_2^I = 4.81 \times 10^{-6}$ min, and $K_2^I = 1.30 \times 10^7$ K^3.

either $T_c \approx 60°C$ or $T_c \approx 70°C$, depending on whether Eq. 13 or 14 was used to fit the data.

Further Discussion of the Temperature Dependence of the Crystallization Half-Time

The most fundamental representation of the bulk crystallization kinetics data is to plot the reciprocal value of the crystallization half-time (i.e., $t_{0.5}^{-1}$) against the crystallization temperature. Figure 7 exhibits a plot of the reciprocal half-time of crystallization data measured using the endothermic technique (see Table 1 and solid circles in Fig. 7) along with those measured using the exothermic technique (see Table 5 in Ref. [20] and open triangles in Fig. 7) as a function of crystallization temperature. Clearly, within the temperature range presented (i.e., $70°C \le T_c \le 105°C$), the bulk crystallization rate, as represented by the value of the reciprocal half-time $t_{0.5}^{-1}$, decreases steadily with an increase in the crystallization temperature.

Since the bulk crystallization rate parameters (e.g., $t_{0.5}^{-1}$) relate, in one way or another, to the primary nucleation rate I and/or the subsequent crystal growth rate G and since the temperature dependence of these microscopic mechanisms are well defined in the literature [23,36,37,39], the temperature dependence of the bulk rate parameter can accordingly be quantified and described. Even though the temperature dependence of the parameters I and G are known to have a different temperature dependence, that is, $I \propto (\Delta T)^{-2}$ and $G \propto (\Delta T)^{-1}$, respectively, the bulk rate parameters have often been taken to have a similar temperature dependence as that of the subsequent crystal growth rate G (written in the context of the original Lauritzen and Hoffman secondary nucleation theory [LH theory] [23,39]), which can be expressed as

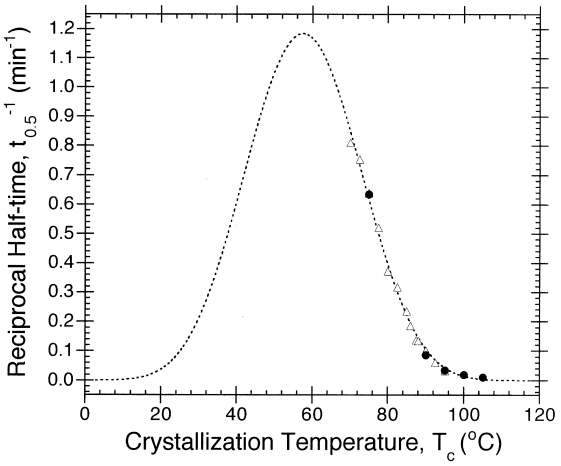

FIG. 7. Reciprocal half-time $t_{0.5}^{-1}$ as a function of crystallization temperature T_c for s-PP. ●, the data measured from this work (see Table 1); △, the data measured from the traditional technique (see Table 5 in Ref. 20). The dotted line is the best-fitted curve drawn through the bulk of the data after Eq. 15. Parameters of the fitted curve: $\Psi_0 = 2.38 \times 10^{12}$ min^{-1} and $K_3^I = 6.38 \times 10^5$ K^2.

$$\Psi(T_c) = \Psi_0 \exp\left[-\frac{U^*}{R(T_c - T_\infty)} - \frac{K_3^I}{T_c(\Delta T)f} \right] \tag{15}$$

where $\Psi(T_c)$ and Ψ_0 are the bulk crystallization rate parameter (e.g., $t_{0.5}^{-1}$) and the preexponential parameter [e.g., $(t_{0.5}^{-1})_0$ (viz. the preexponential factor when Eq. 15 is used to fit the crystallization half-time data)], respectively, k_3^I is a combined factor related to the nucleation mechanism, and the other quantities are the same as previously defined.

With the aid of Eq. 15, the temperature dependence of the bulk rate function $\Psi(T_c)$ can now be quantified by directly fitting the experimental data collected at various crystallization temperatures to Eq. 15 using the same nonlinear multivariable regression program (shown in Fig. 7 as the dotted line). Apparently, the best fit drawn through the bulk of the data exhibits a bell-shaped curve, which is attributed to the nucleation control effect at the high crystallization temperature side (low degrees of undercooling) and the diffusion control effect at the low crystallization temperature side (high degrees of undercooling). Intuitively, from the competing contributions of the transport and nucleation terms, it is expected that a maximum in the composite curve should be observed somewhere between T_∞ and T_m^0. Indeed, such a maximum is clearly distinguishable in Fig. 7 at about 60°C. Though the factors controlling the shape of the curves in Figs. 6 and 7 are the same, the facts that Fig. 6 appears to be U shape and that Fig. 7 appears to be bell shape are due to whether there is a negative sign present within the exponential terms in Eqs. 13 to 15.

CONCLUSIONS

We have demonstrated, at least in the case of s-PP, that DSC can be used to study crystallization behavior and the kinetics of the process of semicrystalline polymers at high crystallization temperatures or at low degrees of undercooling, for which the traditional technique is not applicable, by measuring the enthalpy of fusion $\Delta H_{f,t}$ observed in subsequent melting endotherms after isothermal crystallization for various time intervals at T_c.

The applications of this technique and its advantages over the traditional one can be restated as follows:

1. The induction period can be determined more accurately, and it is taken as the longest time interval the polymer of interest spends at T_c that does not result in the observation of a melting peak in the subsequent melting endotherms.
2. Whether secondary crystallization occurs during the course of crystallization can be determined by observing whether the melting shoulder, which is located close to the crystallization temperature, is shown in the subsequent melting endotherms. The time interval required for the melting shoulder to be observed is taken roughly as the onset (time) of the secondary crystallization.
3. Whether a lamellar thickening process occurs during the course of crystallization can be determined by observing whether the position of the primary melting peak in the subsequent melting endotherms increases with increasing time intervals the polymer of interest spends isothermally at T_c.
4. Related crystallization kinetics parameters can be obtained by analyzing the relative crystallinity data, calculated from the ratio of the enthalpy of fusion measured from subsequent melting endotherms after isothermal crystallization at T_c for various time

intervals to the final value of the enthalpy of fusion, based on an appropriate macrokinetic model.

Disadvantages of the technique are as follows:

1. Accuracy of the relative crystallinity data obtained depends significantly on the choice of the final value of the enthalpy of fusion used. To increase the accuracy of the data, a large number of data points are required, but this has proved to be a very tedious process, especially at very high T_c.
2. It has been shown in the literature that some polymers exhibit a more complex melting behavior than we observed in s-PP, such as in the case of syndiotactic polystyrene (s-PS) [40] and poly(butylene succinate) (PBS) [41]. It is therefore questionable whether the technique will be applicable to describe the crystallization process of those systems, and it should be the subject of future research.

ACKNOWLEDGMENT

We would like to thank Dr. Joseph Schardl of Fina Oil and Chemical Company, Dallas, Texas, for supplying the s-PP resin used in this study and Dr. Roger A. Phillips and his coworkers of Montell USA, Incorporated, Elkton, Maryland, for performing sample characterizations.

REFERENCES

1. B. Wunderlich, *J. Therm. Anal.*, *46*, 643 (1996).
2. J. N. Hay and M. Sabir, *Polymer*, *10*, 203 (1969).
3. J. N. Hay, P. A. Fitzgerald, and M. Wiles, *Polymer*, *17*, 1015 (1976).
4. J. N. Hay, *Br. Polym. J.*, *11*, 137 (1979).
5. P. Supaphol and J. E. Spruiell, *J. Appl. Polym. Sci.*, *75*, 337 (2000).
6. A. N. Kolmogoroff, *Izv. Akad. Nauk USSR, Ser. Math.*, *1*, 355 (1937).
7. W. A. Johnson and K. F. Mehl, *Trans. Am. Inst. Mining Met. Eng.*, *135*, 416 (1939).
8. M. Avrami, *J. Chem. Phys.*, *7*, 1103 (1939).
9. M. Avrami, *J. Chem. Phys.*, *8*, 212 (1940).
10. M. Avrami, *J. Chem. Phys.*, *9*, 177 (1941).
11. U. R. Evans, *Trans. Faraday Soc.*, *41*, 365 (1945).
12. Z. Ding and J. E. Spruiell, *J. Polym. Sci., Polym. Phys.*, *35*, 1077 (1997).
13. M. C. Tobin, *J. Polym. Sci., Polym. Phys.*, *12*, 399 (1974).
14. M. C. Tobin, *J. Polym. Sci., Polym. Phys.*, *14*, 2253 (1976).
15. M. C. Tobin, *J. Polym. Sci., Polym. Phys.*, *15*, 2269 (1977).
16. A. Y. Malkin, V. P. Beghishev, I. A. Keapin, and S. A. Bolgov, *Polym. Eng. Sci.*, *24*, 1396 (1984).
17. P. Supaphol and J. E. Spruiell, *J. Macromol. Sci., Phys., B39*, 257 (2000).
18. B. Wunderlich, in *Macromolecular Physics*, Vol. 2, Academic, New York, 1976, pp. 132–147.
19. W. Banks, A. Sharples, and J. N. Hay, *J. Polym. Sci., A2*, 4059 (1964).
20. P. Supaphol and J. E. Spruiell, *J. Appl. Polym. Sci., 75*, 44 (2000).
21. E. M. Woo and T. Y. Ko, *Colloid Polym. Sci., 274*, 309 (1996).
22. C.-S. Wang, C.-S. Lin, and N. Lai, *Polym. Bull., 39*, 185 (1997).
23. J. D. Hoffman, G. T. Davis, and J. I. Lauritzen, Jr., in *Treatise on Solid State Chemistry*, Vol. 3 (N. B. Hannay, Ed.), Plenum, New York, 1976, chap. 7.
24. J. Schmidtke, G. Strobl, and T. Thurn-Albrecht, *Macromolecules*, *30*, 5804 (1997).

25. G. Hauser, J. Schmidtke, and G. Strobl, *Macromolecules*, *31*, 6250 (1998).
26. T. Hugel, G. Strobl, and R. Thomann, *Acta Polym.*, *50*, 214 (1999).
27. P. Supaphol, *J. Appl. Polym. Sci.*, submitted.
28. H. Janeschitz-Kriegl, *Colloid Polym. Sci.*, *275*, 1121 (1997).
29. H. Janeschitz-Kriegl, E. Ratajski, and H. Wippel, *Colloid Polym. Sci.*, *277*, 217 (1999).
30. F. Lednicky and M. Muchova, *Collect. Czech. Chem. Commun.*, *58*, 2444 (1993).
31. M. Muchova and F. Lednicky, *J. Macromol. Sci., Phys.*, *B34*, 55 (1995).
32. F. Lednicky and M. Muchova, *J. Macromol. Sci., Phys.*, *B34*, 75 (1995).
33. F. Lednicky and M. Muchova, *J. Macromol. Sci., Phys.*, *B35*, 681 (1996).
34. M. Muchova and F. Lednicky, *Polymer*, *37*, 3031 (1996).
35. M. Muchova and F. Lednicky, *Polymer*, *37*, 3037 (1996).
36. F. P. Price, in *Nucleation* (A. C. Zettlemoyer, Ed.), Marcel Dekker, New York, 1969, chap. 8.
37. B. Wunderlich, in *Macromolecular Physics*, Vol. 2, Academic, New York, 1976, chap. 5.
38. T. Suzuki and A. J. Kovacs, *Polymer J.*, *1*, 82 (1970).
39. J. D. Hoffman and R. L. Miller, *Polymer*, *38*, 3151 (1997).
40. E. M. Woo and F. S. Wu, *Macromol. Chem. Phys.*, *199*, 2041 (1998).
41. E. S. Yoo and S. S. Im, *J. Polym. Sci., Polym. Phys.*, *37*, 1357 (1999).

Received February 22, 2000
Revised May 24, 2000
Accepted May 24, 2000

MARCEL DEKKER, INC.
270 Madison Avenue, New York, New York 10016